Changing dynamical control of early Asian summer monsoon in the mid-1990s

Chi-Hua Wu[1] · Pei-Chia Tsai[1] · Nicolas Freychet[2]

Abstract

The seasonal evolution of the upper tropospheric South Asian high follows and influences underlying summer monsoon advancement. A strong connection between the South Asian high and westerly perturbation to the north suggests further planetary-scale dynamical control of the monsoon. In the mid-1990s, a clear location shift of the South Asian high in May–June was noted and was observed in fewer (more) frequencies of the high centers over the Indochina Peninsula (Iranian Plateau). Continental confinement of monsoonal circulation and precipitation was observed during 1995–2010, as opposed to larger-scale development in the Asia–Pacific region during 1979–1994. In view of early-summer monsoon evolution, a westward shifting and faster migration of the South Asian high may imply increased control of the midlatitude dynamics. By contrast, the convection over the tropical Western North Pacific (WNP) has an opposite and delayed contribution to monsoon advancement. After the mid-1990s than it had been previously, the midlatitude jet stream largely weakened over northern Africa and the East Asia–Pacific region, corresponding to an increase in the upper tropospheric geopotential heights north of the jet stream. Climate model experiments further reveal that the warming over Europe–Asia and temperature change in the North Atlantic can result in the change in midlatitude perturbations and the monsoon evolution in the mid-1990s, suggesting large-scale and dynamic impact on monsoon climatology.

Keywords Asian summer monsoon · Decadal change · Monsoon dynamics · Monsoon-midlatitude interaction · South Asian high

1 Introduction

Decadal changes (Yu and Zhou 2007; Ding et al. 2008; Jiang et al. 2008; Zhou et al. 2009b; Li et al. 2010; Turner and Annamalai 2012) in precipitation—whether in pattern shifts or intensity changes—imply that monsoon climatology could be modulated. Existing studies have considered the summer monsoon changes in the 1990s, including a strengthening of the East Asian summer monsoon in the early- to mid-1990s (Liu et al. 2012; Yim et al. 2014); an advanced summer monsoon onset over the Arabian Sea, the Bay of Bengal, and the region around the Philippines

near 10°N in the mid-1990s (Kajikawa et al. 2012); a strengthening of the West African summer monsoon in the late-1990s (Li et al. 2012). Preethi et al. (2017b) examined trends in recent decades over the Asian summer monsoon regions and indicated that the entire monsoon circulation might have shifted westwards. The Afro–Asian monsoon might have shifted to another phase in the early twenty-first century coinciding to the increasing number of record-breaking extreme weather events in recent decades (Barriopedro et al. 2011; Coumou and Rahmstorf 2012). Furthermore, multidecadal variability such as periods with eastward or westward extension of the monsoons have been mentioned regarding a projected future climate change (Preethi et al. 2017a). Recently, emphasis has been placed on understanding a changing linkage between the monsoon subsystems; for example, a strengthened (weakened) linkage of the western Pacific subtropical high to the Indian summer monsoon (East Asian summer monsoon) in the late-1990s (Huang et al. 2018). However, few scientific studies have revealed large-scale effects of monsoon

✉ Chi-Hua Wu
chhwu@gate.sinica.edu.tw

[1] Research Center for Environmental Changes, Academia Sinica, 128 Academia Road, Section 2, Nankang, Taipei 115, Taiwan

[2] School of Geosciences, University of Edinburgh, Edinburgh, UK

seasonality. A comprehensive investigation of changes in seasonal characteristics of monsoons may provide insights into climate dynamics and changes.

The anticyclonic gyre with its center on South Asia (also recognized as the South Asian high) is typical of the boreal-summer intercontinental circulation in the upper troposphere. Seasonal evolution of the massive anticyclone follows and influences the advancement of underlying subtropical monsoons (Liu et al. 2013; Wei et al. 2015; Zhang et al. 2016; Wu et al. 2015, 2018b), which is topographical (Boos and Kuang 2010; Wu et al. 2018a) and can be modulated by midlatitude perturbations (Enomoto 2004; Watanabe and Yamazaki 2012). Investigation of the forcing and response of the upper tropospheric anticyclone could increase understanding of how the summer monsoon changes in a varying climate, particularly with respect to seasonal details.

At the beginning of the Asian summer monsoon (late spring–early summer), the South Asian high migrates northwestward with its center over the Indochina Peninsula and southern Tibetan Plateau. After reaching its northernmost position near 30°N, the high center may oscillate in the longitudes over the Tibetan Plateau and Iranian Plateau in summer through autumn, exhibiting bimodal structures classified as the Tibetan mode (TM) and Iranian mode (IM) (Zhang et al. 2002). In view of a climatological state, stage-wise evolution of the monsoon in a subseasonal timescale is characterized by the distinct modes of the South Asian high. However, the dynamics and driving factors of these upper-level circulation patterns as well as the connections in between are not well understood.

In this study, we investigated the evolution of the South Asian high in May–June during 1979–2010 and focused on its pattern shift in the mid-1990s. In addition to the TM and IM, the Indochina mode (ICM) is also considered a major characteristic of the South Asian high in May–June. We were motivated to explore decadal changes in the seasonal modes of the high, including associated monsoon behaviors and large-scale connections as well as extreme weather events over specific regions. The methods and results can be applied to further improve understanding of the state-dependent sensitivity of monsoon seasonality such as in paleoclimate and modeling studies. The remaining paper is organized as follows: The data and models are described in Sect. 2. Section 3 explores decadal changes in the mid-1990s and examines the existing mechanisms. In Sect. 4, we identify the South Asian high modes, investigate the dynamics in the distinct modes of the high, and explore the changes in seasonal modes in the high. Section 5 discusses forcing mechanisms of the changing early Asian summer monsoon and applications, and Sect. 6 gives concluding remarks.

2 Data and models

Observation and reanalysis data used during 1979–2010 included that of (a) precipitation from the Global Precipitation Climatology Project (GPCP) (Huffman et al. 2001), with a temporal resolution of 1 pentad and 2.5° latitude–longitude spatial resolution; (b) zonal and meridional winds, geopotential heights, and omega from the National Centers for Environmental Prediction (NCEP) reanalysis (Kalnay et al. 1996), with temporal resolution of 6 h and 2.5° latitude–longitude spatial resolution; and (c) daily gridded (1-km resolution) dataset of precipitation in Taiwan (Weng and Yang 2018). The sea surface temperature (SST) data during 1982–2010, with temporal resolution of 1 day and 1° latitude–longitude spatial resolution, from National Oceanic and Atmospheric Administration (NOAA) Optimum Interpolation (OI) analysis (Reynolds et al. 2007) was used as boundary forcing in experimental simulations.

We conducted experimental simulations using a simplified general circulation model to explore and generate fundamental ideas regarding changes in the South Asian high. The eight-layer Simplified Parameterization, privitivE-Equation Dynamics (SPEEDY), coupled with a slab ocean model and equipped with simplified physical parameterizations in a T30 spatial resolution (Molteni 2003; Kucharski et al. 2005), was developed by the International Centre for Theoretical Physics (ICTP). We also examined the South Asian high simulations in six Coupled Model Intercomparison Project Phase 5 (CMIP5) models (historical simulations from 1976 to 2005 were analyzed); we calculated the averaged wind fields within 100–250 hPa since most of the model outputs include only a few layers in the upper troposphere. A summary (model name/institute/country/horizontal resolution) of the used models is listed as follows: (a) BCC-CSM1-1/BCC and CMA/China/64×128; (b) BNU-ESM/Beijing Normal University (BNU)/China/64×128; (c) CanESM2/Canadian Centre for Climate Modeling and Analysis (CCCma)/Canada/64×128; (d) CMCC-CESM/Centro Euro-Mediterraneo per i Cambiamenti Climatici (CMCC)/Italy/48×96; (e) CNRM-CM5/Centre National de Recherches Météorologiques (CNRM), and Centre Européen de Recherches et de Formation Avancée en Calcul Scientifique/France/128×256; (f) MIROC5-ESM-CHEM/Atmosphere and Ocean Research Institute (AORI; The University of Tokyo), National Institute for Environmental Studies (NIES), and Japan Agency for Marine-Earth Science and Technology (JAMSTEC)/Japan/64×128.

3 Decadal changes in the mid-1990s

In May–June, the midlatitude westerly jet stream weakens and migrates northward, corresponding to South Asian high evolution and monsoon advancement. The highest speeds of the upper-level jet stream occur at the northern edge of the South Asian high (Fig. 1a). In the lower troposphere, surrounding the cyclonic streamfunction (monsoon low) over South Asia, anticyclonic streamfunction occurs over the North Pacific, North Atlantic–West Africa, and tropical Indian Ocean regions (Fig. 1b). The westerly jet stream in the upper troposphere is well coupled with the westerly flow in the lower troposphere along the northern edge of the Pacific high, which provides background characteristics of circulation regarding tropical and midlatitude dynamics.

During 1995–2010 relative to 1979–1994, the upper-level jet stream largely weakened over northern Africa and the East Asia–Pacific region; this corresponded to an increase in the upper-level geopotential heights north of the jet stream (Fig. 1c). The South Asian high in May–June was stronger during 1995–2010 than 1979–1994 over the Iranian Plateau, whereas it was weaker over Southeast Asia. In the lower troposphere, anomalously anticyclonic

circulation (streamfunction) can be observed over Eurasia–northern Africa and the North Pacific, and this also corresponds to the weakening of the westerly flow. The anomalously anticyclonic streamfunction over the India–tropical Indian Ocean and WNP regions is notable and corresponds to a weakened monsoon in South Asia and an equatorial confinement of the Pacific high (Fig. 1d). Temporal changes in specific regions have been further examined with respect to upper-level zonal winds (Africa–Europe: 0°–60°E, 30°N–40°N; East Asia: 110°E–140°E, 35°N–45°N; Fig. 2b) and low-level streamfunctions (tropical WNP: 130°E–180°E, 5°N–15°N; tropical Indian Ocean: 60°E–100°E, 5°N–15°N; Fig. 2c). Abrupt changes in the selected circulation fields in the mid-1990s can be clearly identified.

Monsoon changes in the 1990s may have primarily resulted from a change in the land-sea thermal contrast, which involves changes on a global scale [as mechanisms of 'warm land–cold ocean' and 'warm Northern Hemisphere–cold Southern Hemisphere (Wang et al. 2012)] and changes in specific regions such as amplified summer warming in Europe–West Asia and Northeast Asia (Xiaowei et al. 2017) and SST changes in the North Atlantic (Yim et al. 2014). Dynamical connections driven by the changing thermal contrast may involve phase shift in Atlantic
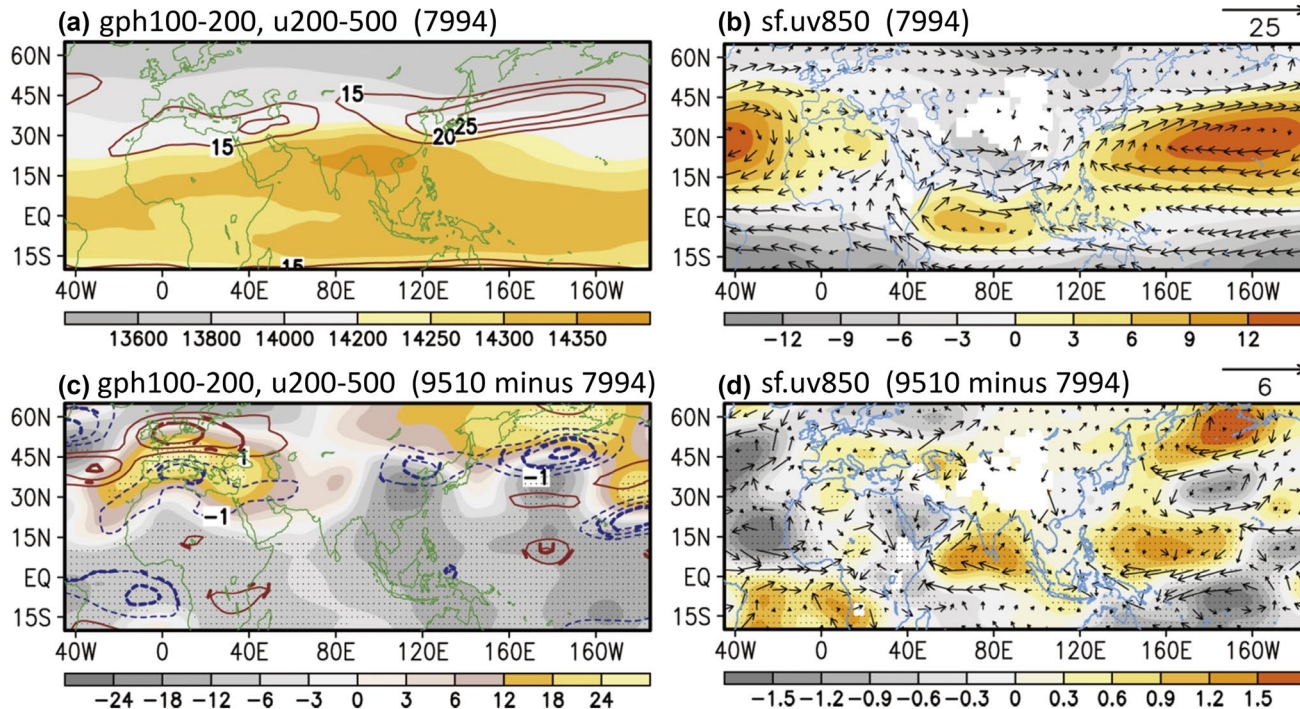

Fig. 1 Climatological mean of **a** geopotential heights within 100–200 hPa (shaded, gpm) and zonal winds within 200–500 hPa (contour lines for speeds higher than 15 m s^{-1}), and **b** streamfunction (shaded, 10^6 m^2 s^{-1}) and winds at 850 hPa during 1979–1994. **c–d** Same as (**a–b**) except during 1995–2010 minus during 1979–1994; thick contour lines (dots) denote that the difference in zonal winds (geopotential heights and streamfunctions) has a confidence level of 90%
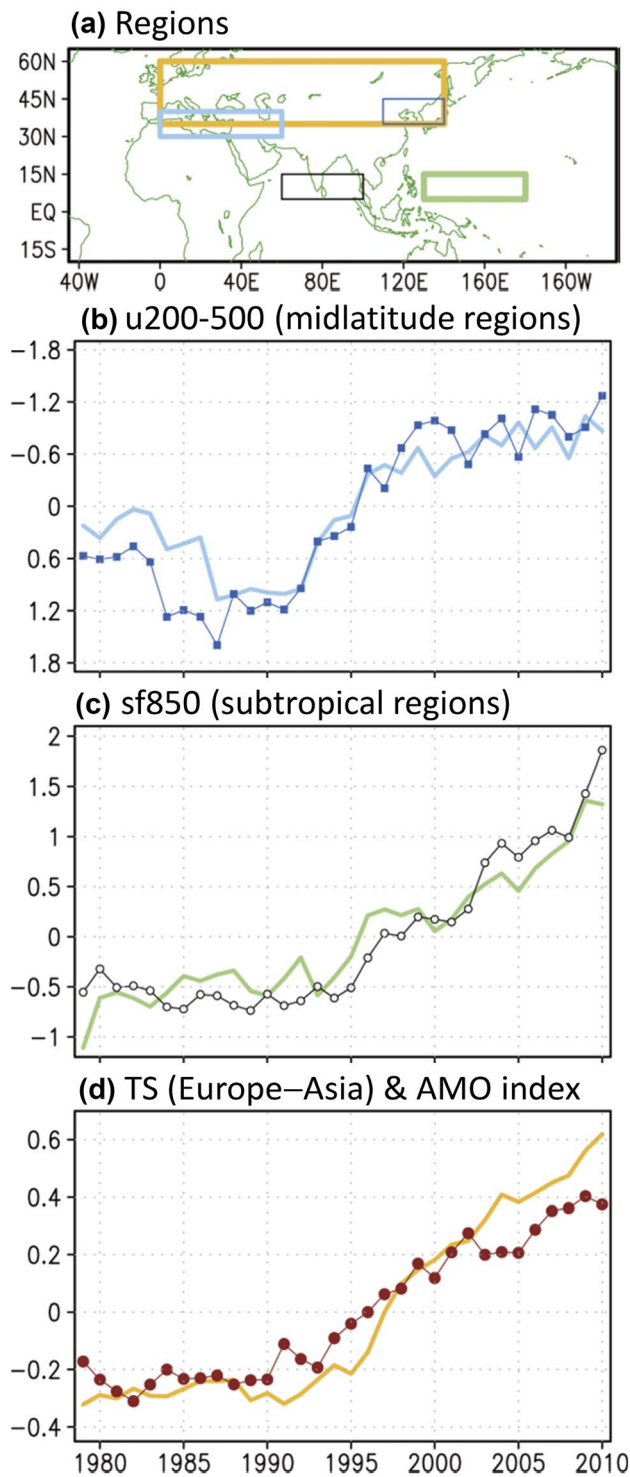
(a) Regions

(b) u200-500 (midlatitude regions)

(c) sf850 (subtropical regions)

(d) TS (Europe–Asia) & AMO index

Fig. 2 Temporal evolution of (**b**) zonal winds within 200–500 hPa (unit: m s^{-1}) over (0°–60°E, 30°N–40°N; thick line) and (110°E–140°E, 35°N–45°N; thin line with squares); **c** the 850-hPa streamfunction (unit: 10^6 m^2 s^{-1}) over (130°E–180°E, 5°N–15°N, thick line) and (60°E–100°E, 5°N–15°N, thin line with circles); and **d** surface air temperature over (0°–140°E, 35°N–60°N, thick line, unit: K) and the AMO index (×2, thin line with dots, unit: K). The average in 1979–2010 was subtracted and 9-year running applied. The analyzed regions were marked in (**a**)
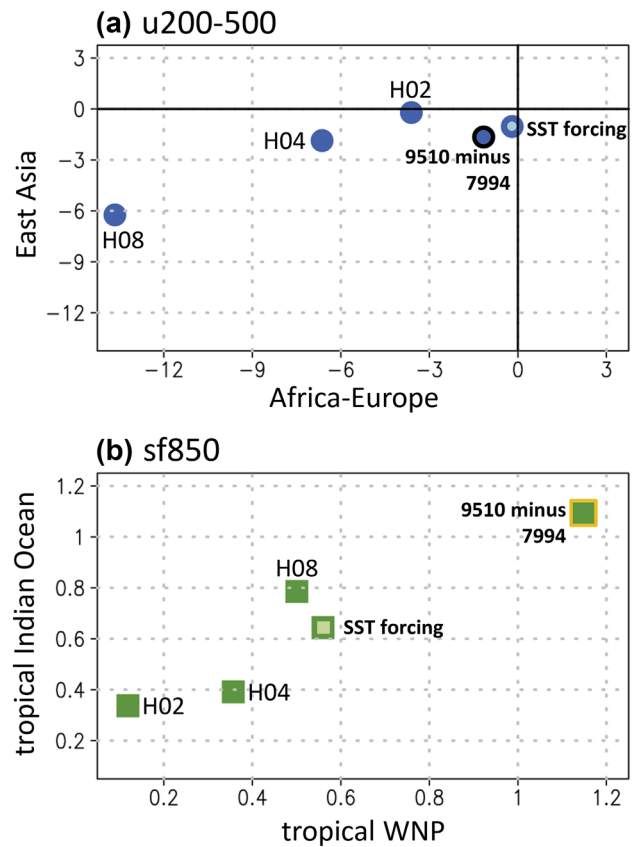
(a) u200-500

(b) sf850

Fig. 3 Responses of (**a**) upper-level (200–500 hPa) zonal winds and (**b**) 850-hPa streamfunctions to a given atmospheric heating forcing (0.2, 0.4, and 0.8 °C day^{-1} were in turn given in the troposphere of Eurasia: 0°–140°E, 35°N–60°N) and SST forcing (observed SST difference between 1982–1994 and 1995–2010). Following Fig. 2, the upper-level wind responses over Africa–Europe (0°–60°E, 30°N–40°N) and East Asia (110°E–140°E, 35°N–45°N) are shown; the lower-level streamfunction response over tropical WNP (130°E–180°E, 5°N–15°N) and tropical Indian Ocean (60°E–100°E, 5°N–15°N) are shown. Observed differences between 1979–1994 and 1995–2010 are also marked in the figures

Multi-decadal Oscillation (AMO) and decadal change in midlatitude perturbations (Yim et al. 2014; Xiaowei et al. 2017). Coinciding to the abrupt changes in upper-level winds and low-level streamfunctions in the focused regions (Fig. 2b–c), abrupt changes in the AMO index (calculated by area-weighted average over the North Atlantic using Kaplan SST dataset) (Enfield et al. 2001) and surface temperature over Eurasia (0°–140°E, 35°N–60°N) in the mid-1990s can be also clearly identified (Fig. 2d).

We further explored and partly confirmed the effects of continental heating and SST on atmospheric circulation (Fig. 3), specifically regarding the responses of upper-level zonal winds and low-level streamfunctions (identification same as Fig. 2) in a simplified general circulation model. The atmospheric heating forcing by 0.2, 0.4, and 0.8 °C day^{-1} were in turn given over Eurasia (0°–140°E,

35°N–60°N) at 300–1000 hPa of the model. The model results confirmed that major changes in circulation (i.e., midlatitude westerlies and tropical streamfunctions) in the mid-1990s can be attributed partly to continental heating changes. Moreover, we explored the SST impact on decadal circulation shifts by conducting an SST anomaly (observed SST difference between 1982–1994 and 1995–2010 as forcing). The results suggest that the upper-level wind changes over East Asia well followed the SST changes, whereas the SST changes may have had a secondary effect on modulating wind changes over Africa–Europe. A substantial impact of SST changes on the tropical streamfunction can be clearly identified.

4 Decadal changes in seasonal modes in the South Asian high

4.1 Identification of South Asian high modes

We defined the South Asian high center based on averaged geopotential heights within 100–200 hPa. For each pentad in the analyzed periods, we first identified the positions (longitudes and latitudes) where the maximum value of the geopotential height existed in a large domain (40°E–140°E, 0°–50°N); in a few rare cases (four pentads during 1979–1994 and two pentads during 1995–2010), the high center was identified on two consecutive grids. The South Asian high modes were identified in longitude. Generally, only 12 cases (the 25th–the 36th pentads) were available for each year in May–June. Regarding South Asian high locations during 1979–1994 and 1995–2010, frequency by 100% was mostly equivalent to 192 pentads by 12 pentads × 16 years. Finally, we defined the IM, TM, and ICM when the high centers occurred at 55°E–65°E, 82.5°E–92.5°E, and 97.5°E–107.5°E, respectively. Composite analysis was conducted based on identification of the high center.

Figure 4a shows all the ICM, TM, and IM cases (pentads) during 1979–2010. Mostly, the ICM occurs earlier and the IM occurs later. During 1979–1994, averaged high centers of 100–200 hPa comprised the ICM by 38%, TM by 17%, and IM by 12% of the total pentads. During 1995–2010, the high centers in May–June comprised the ICM by 21% and the IM by 18% of the analyzed data, revealing a lower frequency in the ICM and higher frequency in the IM compared with 1979–1994 (Fig. 4b). The geopotential heights that averaged 100–200 hPa were analyzed to gain an overall structure of the upper-level anticyclone; the physical details regarding a cold high at 100 hPa and a warm high beneath may have been involved in combination. Zonal distribution of the 100-hPa high centers following existing studies (Zhang et al. 2002; Zhou et al. 2009a) was compared (Fig. 4c) and

major types of high center locations were similar to those averaging 100–200 hPa.

The frequency of the ICM in May decreased from 54% during 1979–1994 to 31% during 1995–2010, constituting a reduction of approximately 43% (a decrease from 22% to 11% in June constituted a reduction by half; Fig. 4d, e). Notably, no IM was present in May during 1979–1994, whereas it occurred by 10% during 1995–2010. Furthermore, the high centers during 1995–2010 may have shifted farther westward than they had during 1979–1994. As demonstrated herein, the dynamical control of the IM may differ from that of the ICM. The large contrast in occurrence of the IM and ICM might be related to a changing large-scale condition followed by a pattern shift of monsoon precipitation.

4.2 Dynamics in the distinct modes of the South Asian high (1979–1994)

When the South Asian high is located as the ICM with a high center approximately over 20°N (Fig. 5a), monsoon precipitation mostly occurs over the northeastern Bay of Bengal, the Indochina Peninsula, and subtropical East Asia (110°E–140°E). The earliest Asian summer monsoon including pre-Meiyu (Wu et al. 2014) may have been displayed to a large extent. Vertical coupling of the westerly stream has been emphasized in the early summer monsoon with dramatic effects of topography and involving southwesterly monsoon flow in the lower troposphere, monsoon trough formation in the mid-troposphere, and the South Asian high and westerly jet stream to the north in the upper troposphere (Wu et al. 2014; Wu and Hsu 2016).

In the TM with a high center approximately over 25°N (Fig. 5b), monsoon precipitation increases and expands farther northward compared with the ICM condition, alongside dramatic topographical effects. Corresponding to the strengthening of the monsoon, low geopotential heights (mid-to-lower troposphere) and strong upward motion can be observed over the Bay of Bengal and Tibetan Plateau (82.5°E–92.5°E, 5°N–40°N; Fig. 5d). Regarding seasonal evolution from the ICM to the TM, enhancement of the upper-level high is closely related to the strengthening of the ascending flow and monsoon low (decrease in geopotential heights) in the southern Tibetan Plateau and northern Bay of Bengal (Fig. 5e).

Corresponding to the IM condition, the upper-level high center is located at 25°N–30°N and may be not directly driven by the underlying monsoonal heating. Overall, distribution of monsoonal precipitation in the IM is similar to that in the TM. Small or even no precipitation can be observed over the Iranian Plateau (Fig. 5c). Over the Arabian Sea and Iranian Plateau (55°E–65°E), an ascending flow occurs below 600 hPa at 20°N–40°N, whereas subsidence is strong in the mid-to-upper troposphere over the Iranian Plateau
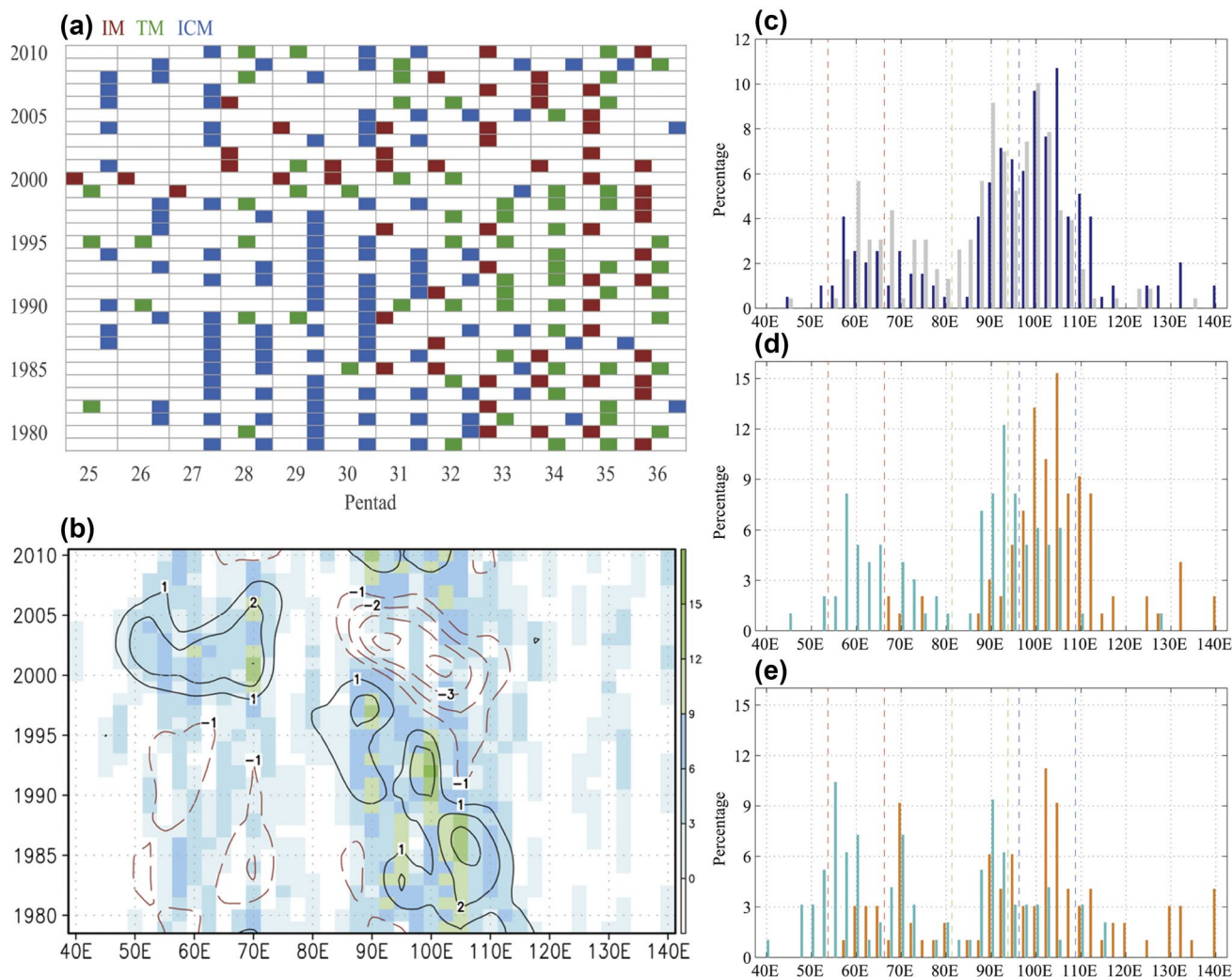
Fig. 4 a The pentads identified as ICM (blue), TM (green), and IM (red) in May–June during 1979–2010 (the 25th pentad: May 1–5; see identification of the high center position in the text). **b** Locations in longitudes (pentad average) of the South Asian high center within 100–200 hPa in May–June for each year (100% is equivalent to 12 pentads); contour lines denote that a long-term average (1979–2010) is subtracted over each longitude position; a 5-year running mean was applied. **c** Locations in longitudes of the South Asian high center in May–June during 1979–1994 (100% is equivalent to 192 pentads by 12 pentads × 16 years). The blue bars denote the high within 100–200 hPa and the gray bars denote the high at 100 hPa. **d** Same as (**c**) except for May (orange) and June (light blue), separately. **e** Same as (**d**) except for 1995–2010. The results of 100–200 hPa are shown in (**d–e**). Dashed lines in (**c–e**) denote the identified longitudes of the IM (55°E–65°E), TM (82.5°E–92.5°E), and ICM (97.5°E–107.5°E), respectively

(Fig. 5f). Over the Iranian Plateau (~ 30°N), the descending motion has the largest decrease in the mid-to-upper troposphere (rather than a homogeneous decrease in the whole troposphere) under the IM condition compared with the TM condition (Fig. 5g). A diagnosis for the atmospheric condition at the IM (Zhang et al. 2002) suggests that the IM can be driven by diabatic heating in the free atmosphere over in situ heating near the surface. According to the literature and our analyses, we postulate that the perturbations in the midlatitudes drive the IM condition and modulate the South Asian high location. A large-scale forcing on the IM provides a perspective to understand scale interaction (synoptic and weather to monsoon and planetary scales) over the monsoon region.

4.3 Changes in seasonal migration (modes) of the South Asian high

In May–June, upper tropospheric divergent winds are strong over the Asian–Pacific region east of the Arabian Sea in association with monsoonal precipitation in South and East Asia as well as tropical convection (Fig. 6a). Correspondingly, convergent winds occur over the African–Atlantic region and exhibit a planetary-scale dipole pattern in the
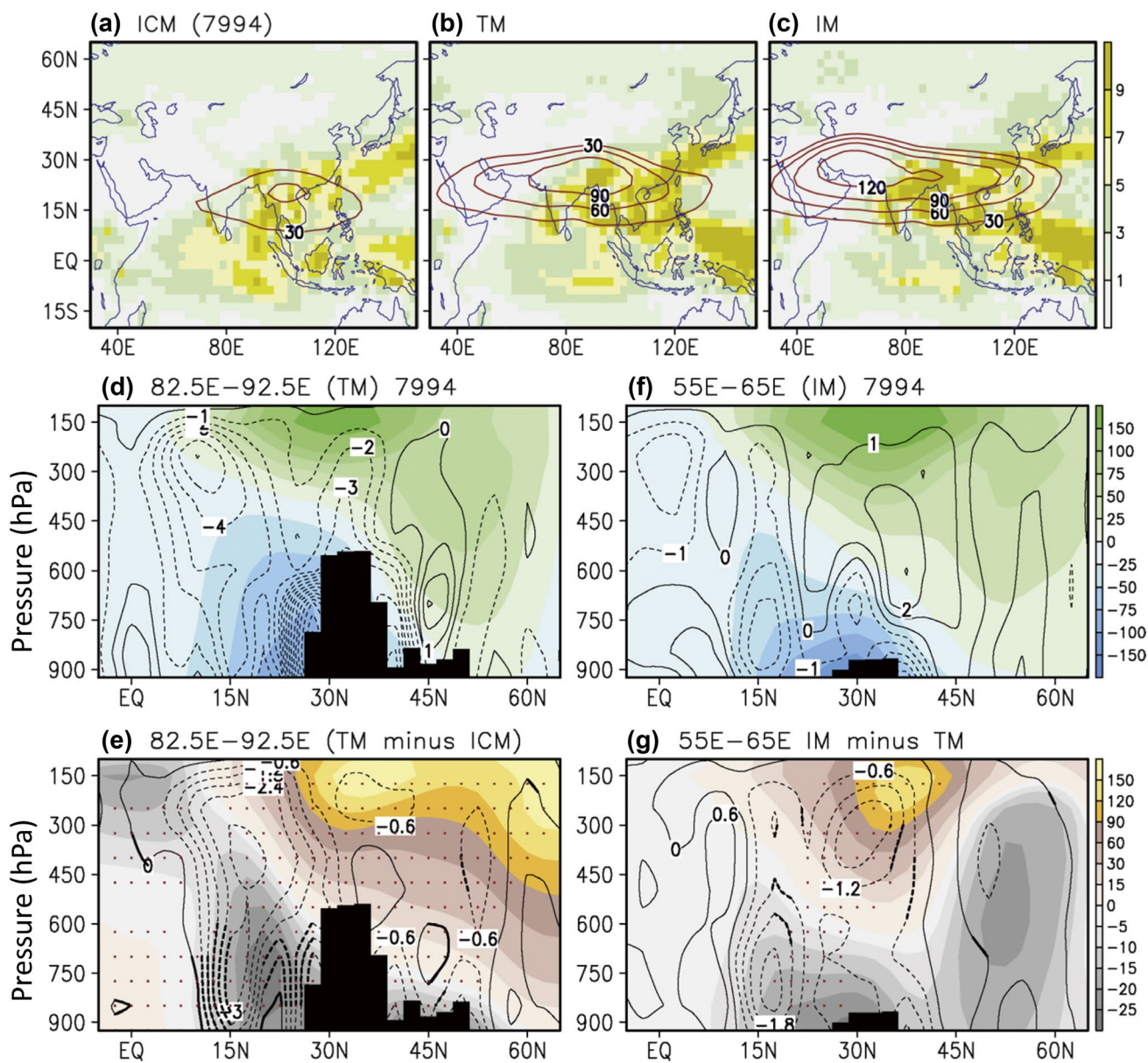
Fig. 5 a–c Precipitation (shaded, mm day^{-1}) and geopotential heights in 100–200 hPa (contour lines, the value 14,300 gpm was subtracted and only results higher than 0 are shown) for the ICM, TM, and IM during 1979–1994. **d–e** Vertical distribution of eddy geopotential heights (shaded, the globally zonal mean is subtracted) and vertical motion (contour lines, Pa min^{-1}) of the TM and the TM minus the ICM at 82.5°E–92.5°E during 1979–1994. **f–g** Same as (**d–e**) except the IM and the IM minus the TM at 55°E–65°E. Thick contour lines (dots) denote that the difference in vertical motion (geopotential heights) has a confidence level of 90% (based on Student's-t test)

upper troposphere. The strength of the dipole structure weakened during 1995–2010 relative to 1979–1994, as shown in the upper-level velocity potentials. The divergent circulation to the east and convergent circulation to the west coincidently weakened (Fig. 6b). We further examined the changes between the South Asian high modes (from the ICM across the TM to IM), which largely represent potential contrasts in seasonal migration. During 1979–1994, precipitation largely increased from the ICM to the TM over South Asia, East Asia, and the tropical WNP. Corresponding to this

large increase in precipitation was a sizable strengthening of divergent circulation in the upper troposphere, with the largest change over Taiwan and the Philippines (Fig. 6c). During 1995–2010, a large increase in precipitation was also observed over South and East Asia in the TM compared with the ICM. However, precipitation decreased over the tropical WNP and South China Sea (Fig. 6d). Corresponding to these precipitation changes, divergent circulation strengthened primarily over South and East Asia, suggesting continental confinement. Regarding the subseasonal shift from the ICM
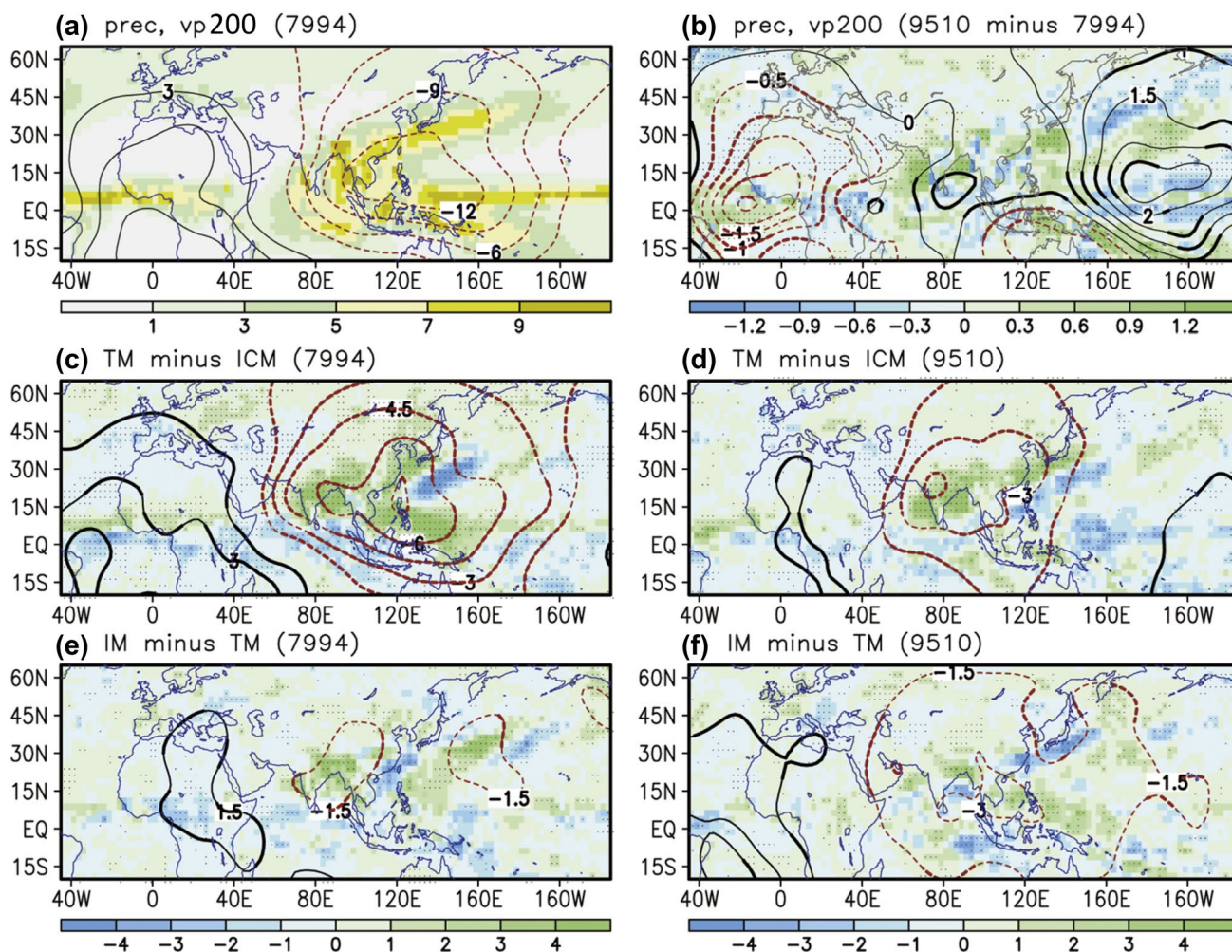
Fig. 6 Precipitation (shaded, mm day^{-1}) and 200-hPa velocity potential (contour lines, 10^6 m^2 s^{-1}) of **a** climatological mean during 1979–1994, **b** climatological mean during 1995–2010 minus that during 1979–1994, **c** TM minus ICM during 1979–1994, **d** TM minus ICM during 1995–2010, **e** IM minus TM during 1979–1994, and **f** IM minus TM during 1995–2010. Thick contour lines (dots) denote that the difference in velocity potentials (precipitation) has a confidence level of 90%

to TM state, synchronous monsoonal development on a large scale occurred during 1979–1994 but disappeared during 1995–2010.

Regarding the IM compared with the TM, regional contrasts in upper-level velocity potential and precipitation were observed during 1979–1994; one example was an increase in precipitation over South Asia (Fig. 6e). By contrast, during 1995–2010, precipitation largely increased over the tropical WNP and large-scale strengthening of the upper tropospheric velocity potential remained evident in the IM relative to the TM (Fig. 6f). We postulate that the convection over the tropical WNP had an opposite (TM vs. ICM) and delayed (IM vs. TM) contribution to the advancement of the early-summer monsoon after rather than before the mid-1990s.

To explore decadal changes in seasonal (subseasonal) states, we examined precipitation and atmospheric circulation differences in the corresponding South Asian high modes individually between 1979–1994 and 1995–2010 (not shown in the figure). Relative to 1979–1994, precipitation during 1995–2010 increased in the ICM over the tropical West Pacific and tropical Atlantic Oceans; this corresponded to a minor increase in the upper-level divergent velocity potential. In the TM and IM during 1995–2010 compared with 1979–1994, precipitation increased over Africa and the tropical Indian Ocean but decreased over subtropical South Asia and the West Pacific. These precipitation changes in the TM and IM corresponded to a large-scale dipole structure in the upper troposphere and Walker-type anomalous circulation (with ascending motion over the Atlantic Ocean–Africa region and descending motion over the South Asia–West Pacific region; not shown in the figure). The weakening of the dipole structure in the upper troposphere particularly in the TM and IM may have made a

major contribution to contrasts between climatological patterns (Fig. 6b).

4.4 Changes in ICM versus IM

In 1979–1994 compared with 1995–2010, the South Asian high centers were located more frequently in the ICM (38% versus 21%) and less frequently in the IM (12% versus 18%). Figure 7 further illustrates the difference in atmospheric conditions between the IM and ICM. Relative to the ICM condition at the beginning of the monsoon, the IM condition was influenced by stronger monsoonal heating with midlatitude modulation. During 1979–1994, at the IM relative to the ICM, precipitation largely increased over South Asia, East Asia, and the tropical WNP, whereas it decreased over the equatorial Atlantic Ocean and Africa and the tropical Indian Ocean. Correspondingly, sizable strengthening of the upper tropospheric divergent circulation occurred over the Asia–WNP domain (Fig. 7a). Furthermore, in the upper troposphere, the geopotential heights (100–200 hPa) increased to nearly zonally uniform in the higher latitudes; this coincided with the largest decrease in zonal winds (200–500 hPa) in the subtropical regions (also zonally uniform; Fig. 7b). In the lower troposphere, a large increase in the monsoonal southerlies and westerlies was observed over South and East Asia; this corresponded to a cyclonic streamfunction anomaly (Fig. 7c).
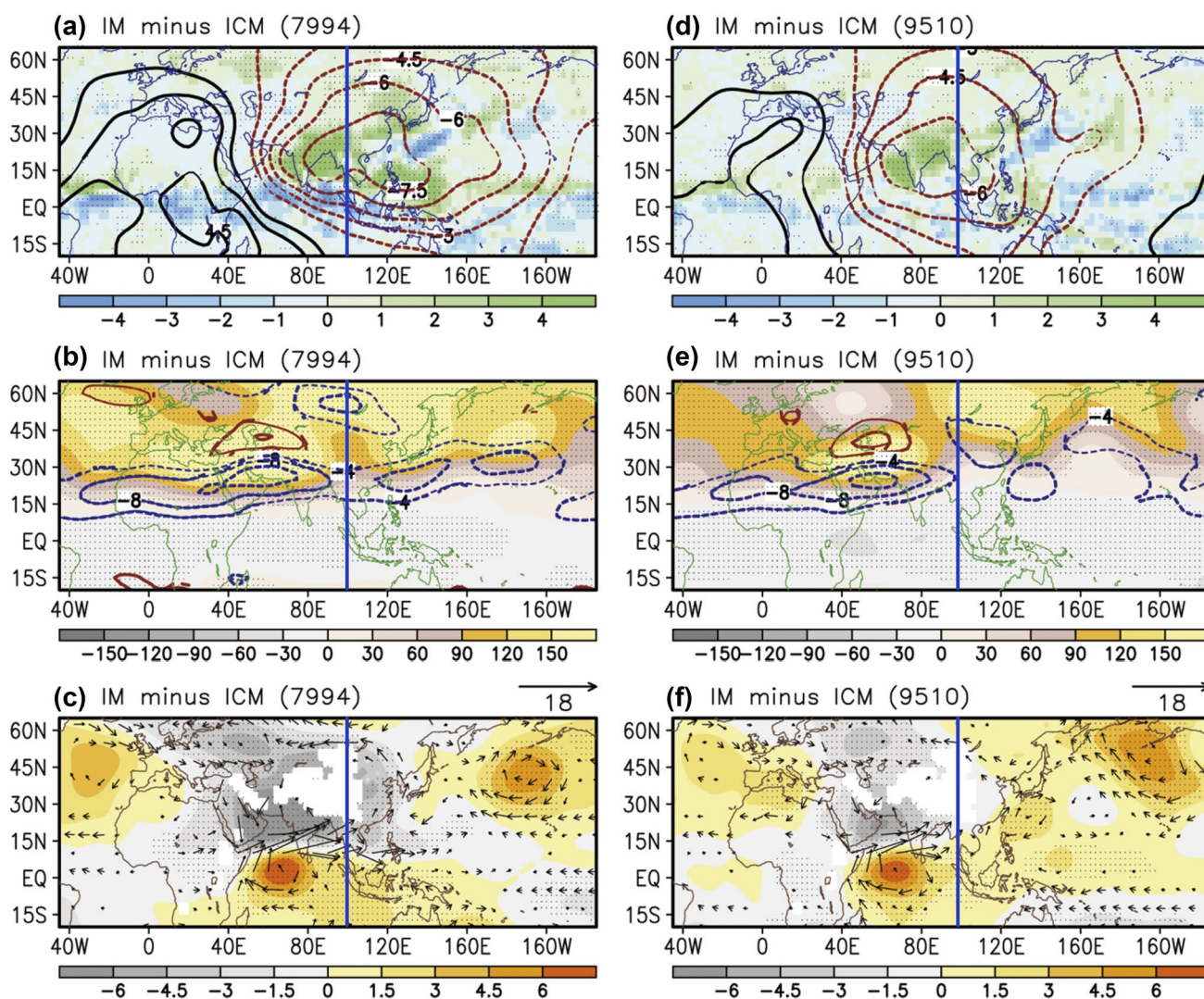

Fig. 7 Difference in **a** precipitation (shaded, mm day^{-1}) and 200-hPa velocity potential (contour lines, 10^6 m^2 s^{-1}), **b** geopotential heights within 100–200 hPa (shaded, gpm) and zonal winds in 200–500 hPa (contour lines, m s^{-1}), and **c** streamfunction (shaded, 10^6 m^2 s^{-1}) and winds at 850 hPa between the IM and ICM during 1979–1994.

d–f Same as (**a–c**) except for 1995–2010. Thick contour lines (dots) denote that the difference in velocity potentials and zonal winds (precipitation, geopotential heights, and streamfunctions) has a confidence level of 90%. Reference lines (blue) were given over 100°E

We focus on seasonal migration between the IM and ICM during 1995–2010 and highlight visible contrasts in conditions during 1979–1994. Comparably, only slight changes in tropical precipitation occurred. With a general increase in precipitation over South and East Asia, smaller and weaker strengthening of the upper-level divergent circulation was observed in seasonal migration (IM minus ICM; Fig. 7d). Large contrasts in seasonal migration were further observed in the East Asia–WNP region (east of 100°E). In the upper troposphere, the increase in geopotential height and decrease in zonal winds exhibited a northeast-southwest tilt rather than being zonally uniform (Fig. 7e). An anticyclonic streamfunction anomaly in the lower troposphere corresponded to weak changes in upper-level circulation (Fig. 7f). Notably, the eastward strengthening of low-level westerly flow in the tropical WNP during 1979–1994 was unobservable during 1995–2010; strengthening of the lower-level negative streamfunction was likely confined west of 100°E (compare Fig. 7c, f).

## 5 Discussions (mechanism and application)

Related studies have indicated that the eastward (westward) shift of the South Asian high accompanies the southward (northward) move in the interannual timescale; the southeast-northwest variation of the high may closely reflect changes in the seasonal modes. The interannual variation of the high position has been suggested to correspond to the strength of the underlying monsoon and suppress the surrounding monsoons (Wei et al. 2015; Zhang et al. 2016; Li et al. 2018). In addition to the traditional view of monsoon seasonality, which considers only thermal heating and/or wind-topography interaction over monsoonal regions, climate model including the larger-scale and midlatitude modulation would have a more realistic monsoon simulation. Insight from large-scale regulation on seasonal details might be crucial for seasonal prediction.

Further sensitivity tests that explore vorticity forcing and responses (observed vorticity difference at 200 hPa between 1979–1994 and 1995–2010 as forcing in a barotropic model) suggest a strong connection between the IM and the TM/ICM. As shown in Fig. 8, an intensified IM suppresses the high (negative vorticity) to the east and southeast, whereas an intensified ICM has a secondary effect on the IM. We therefore suggest that under a large scale control, with a stronger midlatitude modulation, the more frequencies of the South Asian high centers over the Iranian Plateau can dynamically contribute to fewer frequencies of the high centers over the Indochina Peninsula. The midlatitude influence on modulating the locally thermal control of the early summer monsoon may have been implied.

Besides, uncertainty has been noted when studying the bimodality feature of the high using distinct reanalysis

Fig. 8 Vorticity response (contour lines, 10^{-6} s^{-1}; 10th minus 1st day) to a given perturbation (shaded, 10^{-6} s^{-1}) over the **a** Iranian Plateau and **b** Indochina Peninsula within 100–200 hPa. A barotropic model was used
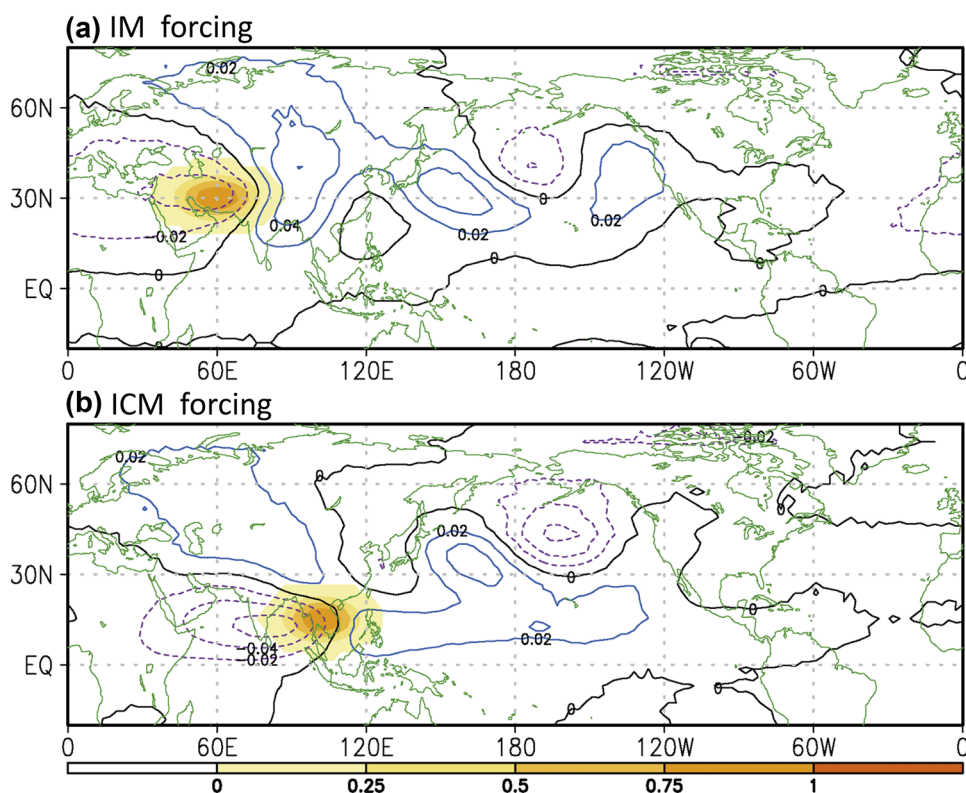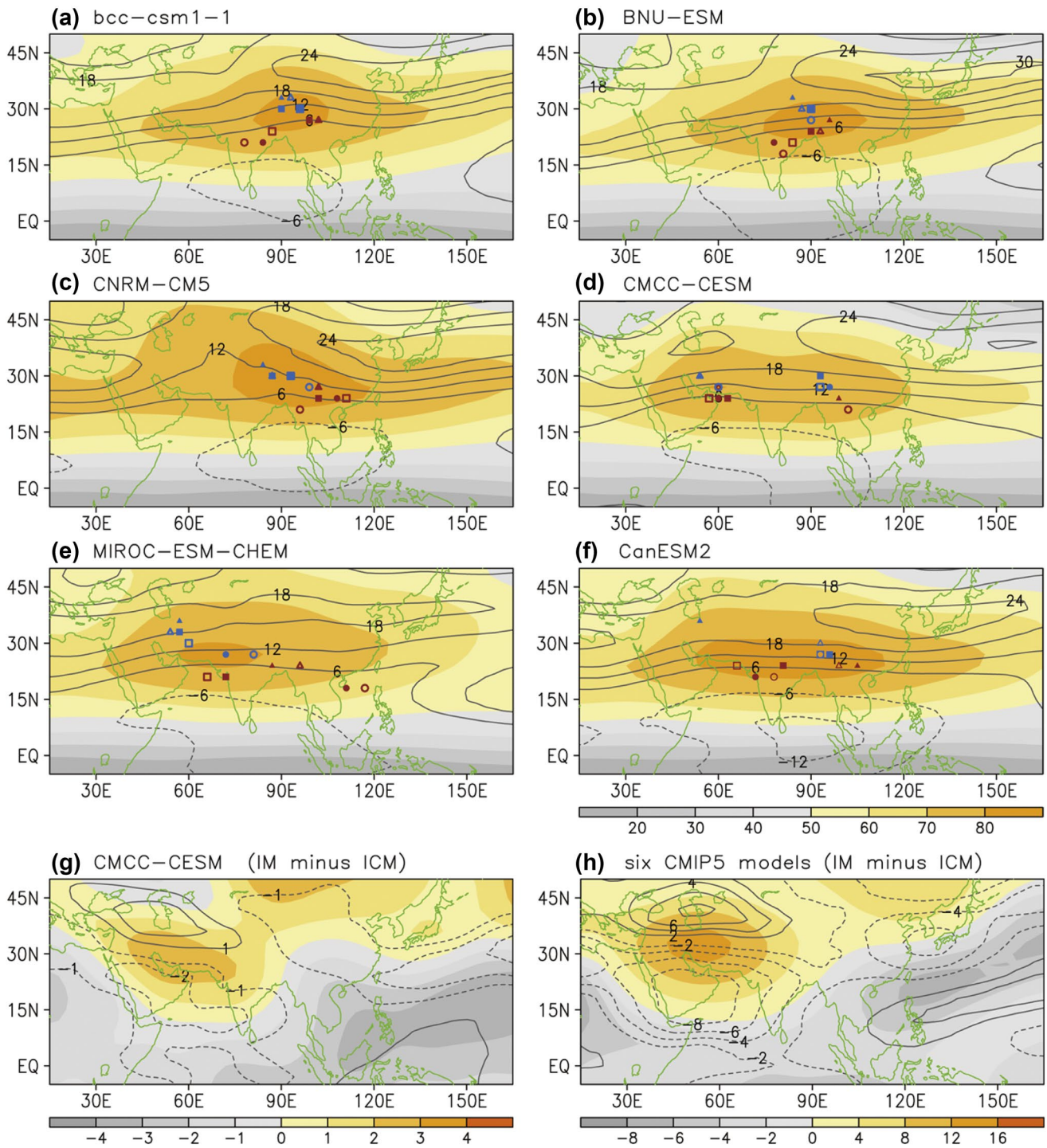
Fig. 9 a–f Mean streamfunctions (shading, 10^6 m² s⁻¹) and zonal winds (contours, m s⁻¹) within 100–250 hPa of six CMIP5 models. Red/blue marks denote the pentad locations of the high center (maximum values in streamfunction were based) in May/June. **g** Differ-ence of streamfunctions and zonal winds between IM and ICM for results of an individual model (CMCC–CESM). Same as (**h**) except for results of multimodel composite

data (Nutzel et al. 2016). Because modeling results are commonly included in reanalysis data, we were moti-vated to search for an insight into climate modeling. We examined six historical simulations in CMIP5. Figure 9 examined mean streamfunctions and zonal winds within 100–250 hPa. The selected models can at least perform meridional advancement of the South Asian high in May (red symbols) and June (blue symbols). Some models can

better simulate the northwestward migration of the high. Following the identification of the ICM and IM in this study, we further examined the contrasts in circulation between the IM and ICM in an individual model (Fig. 9g) and in multi-model ensemble (Fig. 9h), separately. The modeling results well capture the midlatitude perturbation when compared between IM and ICM (refers to Fig. 7b, e). Nevertheless, a disagreement regarding the simulated high center locations remains unresolved, with respect to seasonal evolution and the mean (Figs. 9a–f). It was not in the scope of the present study to comment on model biases. However, attributing dynamical control of simulated monsoon evolution on the subseasonal timescale is worthy of further diagnostic analysis, specifically regarding upper-level high evolution.

We further noted downstream influence of the changing South Asian high on precipitation in Taiwan (application). Taiwan is located at 119°E–122°E and 21°N–25°N and has the Central Mountain Range extending from north to the south of the island. The Meiyu season in Taiwan occurs in May–June corresponding to the early Asian summer monsoon; during the Meiyu, the lower-tropospheric southerlies largely increase, resulting from the strengthening of the WNP high and resulting in large precipitation west of the mountain range (Fig. 10a). During 1995–2010 relative to 1979–1994, associated with a lower frequency in the ICM and higher frequency in the IM, the South Asian high was weaker over Southeast Asia (Fig. 1c). The equatorial confinement of the Pacific high (Fig. 1d) strengthened the lower-tropospheric southwesterly winds and increased
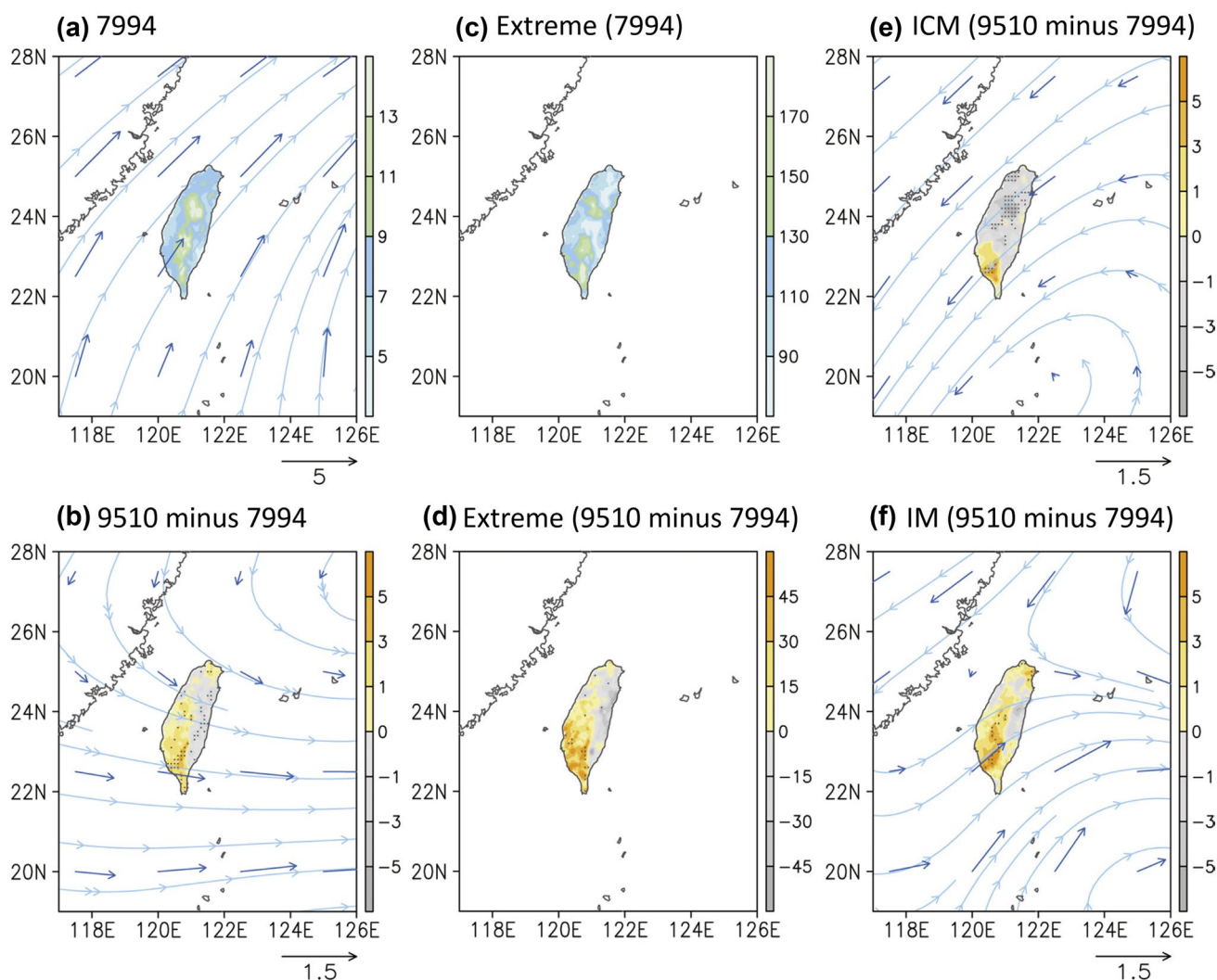

Fig. 10 Precipitation (shaded, mm day^{-1}) and 850-hPa winds (streamlines and vectors, m s^{-1}) of **a** climatological mean during 1979–1994 and **b** climatological mean during 1995–2010 minus that during 1979–1994. **c** Extreme precipitation (95% as threshold) during 1979–1994. **d** Same as (**c**) except for 1995–2010 minus 1979–1994. **e–f** Same as (**b**) except for ICM and IM, respectively. Dots denote that the difference in precipitation has a confidence level of 90%

precipitation over southwestern Taiwan (Fig. 10b). Notably, the circulation changes in the mid-1990s substantially influenced the extreme precipitation (95% as a threshold, Fig. 10c, d; similar results were observed when using 99% as a threshold). The changes in the IM (ICM) condition could have a substantial (secondary) contribution to precipitation in Taiwan (Fig. 10e, f), including the extreme precipitation in the individual mode (not shown in the figure).

Furthermore, changes in the South Asian high were evident in the late-1970s. When expanding the plotting of Fig. 4a–b to the 1950s (not shown), the TM frequency was relatively high prior to the late 1970s compared with the other periods. The ICM and IM occurred more frequently during 1979–1994 and 1995–2010, respectively. Further comparison and exploration of dynamical contrasts between the distinct decadal changes (i.e., late 1970s and mid-1990s) of the South Asian high—particularly with respect to the pattern shifts of the high—could provide an avenue to understanding climate forcing on synoptic even weather scale changes.

6 Concluding remarks

This study noted a clear location shift of the South Asian high in May–June in the mid-1990s, which was observed in fewer (more) frequencies of the high centers over the Indochina Peninsula (Iranian Plateau). During 1995–2010, the monsoon may have exhibited faster advancement despite being weaker than during 1979–1994. Continental confinement of monsoonal circulation and precipitation was observed during 1995–2010 as opposed to larger-scale development in the Asia–Pacific region during 1979–1994. Therefore, the early-summer Asian monsoon—particularly its subseasonal migration and dynamics of the high over and around the Iranian Plateau—likely underwent increasing modulation of the midlatitude and larger-scale dynamics in the mid-1990s.

Climate model experiments suggested that the more frequencies of the South Asian high centers over the Iranian Plateau may dynamically contribute to fewer frequencies of the high centers over the Indochina Peninsula. The midlatitude influence on modulating the locally thermal control of the early summer monsoon was therefore considered. The modeling results further confirmed that the circulation changes in the mid-1990s, including changes in the midlatitude westerlies and tropical streamfunctions, can be attributed to continental heating (i.e. the warming over Europe–Asia) and SST (relates primarily to the North Atlantic forcing) changes.

References

Barriopedro D, Fischer EM, Luterbacher J, Trigo RM, Garcia-Herrera R (2011) The hot summer of 2010: redrawing the temperature record map of Europe. Science 332:220–224. https://doi.org/10.1126/science.1201224

Boos WR, Kuang Z (2010) Dominant control of the South Asian monsoon by orographic insulation versus plateau heating. Nature 463:218–222. https://doi.org/10.1038/nature08707

Coumou D, Rahmstorf S (2012) A decade of weather extremes. Nat Clim Change 2:491–496. https://doi.org/10.1038/Nclimate1452

Ding YH, Wang ZY, Sun Y (2008) Inter-decadal variation of the summer precipitation in East China and its association with decreasing Asian summer monsoon. Part I: observed evidences. Int J Climatol 28:1139–1161. https://doi.org/10.1002/joc.1615

Enfield DB, Mestas-Nuñez AM, Trimble PJ (2001) The Atlantic multidecadal oscillation and its relation to rainfall and river flows in the continental U.S. Geophys Res Lett 28:2077–2080. https://doi.org/10.1029/2000gl012745

Enomoto T (2004) Interannual variability of the Bonin high associated with the propagation of rossby waves along the Asian jet. J Meteorol Soc Jpn 82:1019–1034. https://doi.org/10.2151/jmsj.2004.1019

Huang Y, Wang B, Li X, Wang H (2018) Changes in the influence of the western Pacific subtropical high on Asian summer monsoon rainfall in the late 1990s. Clim Dyn 51:443–455. https://doi.org/10.1007/s00382-017-3933-1

Huffman GJ, Adler RF, Morrissey MM, Bolvin DT, Curtis S, Joyce R, McGavock B, Susskind J (2001) Global precipitation at one-degree daily resolution from multisatellite observations. J Hydrometeorol 2:36–50. https://doi.org/10.1175/1525-7541(2001)002%3c0036:Gpaodd%3e2.0.Co;2

Jiang Z, Yang S, He J, Li J, Liang J (2008) Interdecadal variations of East Asian summer monsoon northward propagation and influences on summer precipitation over East China. Meteorol Atmos Phys 100:101–119. https://doi.org/10.1007/s00703-008-0298-3

Kajikawa Y, Yasunari T, Yoshida S, Fujinami H (2012) Advanced Asian summer monsoon onset in recent decades. Geophys Res Lett. https://doi.org/10.1029/2011gl050540

Kalnay E, Kanamitsu M, Kistler R, Collins W, Deaven D, Gandin L, Iredell M, Saha S, White G, Woollen J, Zhu Y, Chelliah M, Ebisuzaki W, Higgins W, Janowiak J, Mo KC, Ropelewski C, Wang J, Leetmaa A, Reynolds R, Jenne R, Joseph D (1996) The NCEP/NCAR 40-year reanalysis project. Bull Am Meteorol Soc 77:437–471. https://doi.org/10.1175/1520-0477(1996)077%3c0437:Tnyrp%3e2.0.Co;2

Kucharski F, Molteni F, Bracco A (2005) Decadal interactions between the western tropical Pacific and the North Atlantic Oscillation. Clim Dyn 26:79–91. https://doi.org/10.1007/s00382-005-0085-5

Li J, Wu Z, Jiang Z, He J (2010) Can global warming strengthen the East Asian summer monsoon? J Clim 23:6696–6705. https://doi.org/10.1175/2010jcli3434.1

Li H, Wang H, Yin Y (2012) Interdecadal variation of the West African summer monsoon during 1979–2010 and associated variability. Clim Dyn 39:2883–2894. https://doi.org/10.1007/s00382-012-1426-9

Li H, He S, Fan K, Wang H (2018) Relationship between the onset date of the Meiyu and the South Asian anticyclone in April and

the related mechanisms. Clim Dyn. https://doi.org/10.1007/s0038 2-018-4131-5

Liu HW, Zhou TJ, Zhu YX, Lin YH (2012) The strengthening East Asia summer monsoon since the early 1990s. Chin Sci Bull 57:1553–1558. https://doi.org/10.1007/s11434-012-4991-8

Liu BQ, Wu GX, Mao JY, He JH (2013) Genesis of the South Asian high and its impact on the Asian summer monsoon onset. J Clim 26:2976–2991. https://doi.org/10.1175/Jcli-D-12-00286.1

Molteni F (2003) Atmospheric simulations using a GCM with simplified physical parametrizations. I: model climatology and variability in multi-decadal experiments. Clim Dyn 20:175–191. https://doi.org/10.1007/s00382-002-0268-2

Nutzel M, Dameris M, Garny H (2016) Movement, drivers and bimodality of the South Asian High. Atmos Chem Phys 16:14755–14774. https://doi.org/10.5194/acp-16-14755-2016

Preethi B, Mujumdar M, Prabhu A, Kripalani R (2017a) Variability and teleconnections of South and East Asian summer monsoons in present and future projections of CMIP5 climate models. Asia-Pac J Atmos Sci 53:305–325. https://doi.org/10.1007/s1314 3-017-0034-3

Preethi B, Mujumdar M, Kripalani RH, Prabhu A, Krishnan R (2017b) Recent trends and tele-connections among South and East Asian summer monsoons in a warming environment. Clim Dyn 48:2489–2505. https://doi.org/10.1007/s00382-016-3218-0

Reynolds RW, Smith TM, Liu C, Chelton DB, Casey KS, Schlax MG (2007) Daily high-resolution-blended analyses for sea surface temperature. J Clim 20:5473–5496. https://doi.org/10.1175/2007j cli1824.1

Turner AG, Annamalai H (2012) Climate change and the South Asian summer monsoon. Nat Clim Change 2:587–595. https://doi.org/10.1038/Nclimate1495

Wang B, Liu J, Kim H-J, Webster PJ, Yim S-Y (2012) Recent change of the global monsoon precipitation (1979–2008). Clim Dyn 39:1123–1135. https://doi.org/10.1007/s00382-011-1266-z

Watanabe T, Yamazaki K (2012) Influence of the anticyclonic anomaly in the subtropical jet over the western tibetan plateau on the intraseasonal variability of the summer Asian monsoon in early summer. J Clim 25:1291–1303. https://doi.org/10.1175/Jcli-D-11-00036.1

Wei W, Zhang RH, Wen M, Kim BJ, Nam JC (2015) Interannual variation of the South Asian high and its relation with indian and east asian summer monsoon rainfall. J Clim 28:2623–2634. https://doi.org/10.1175/Jcli-D-14-00454.1

Weng S-P, Yang C-D (2018) The construction and verification of daily gridded rainfall dataset (1960–2015) in Taiwan. Taiwan Water Conserv 66:33–52

Wu C-H, Hsu H-H (2016) Role of the Indochina Peninsula narrow mountains in modulating the East Asian-Western North Pacific

summer monsoon. J Clim 29:4445–4459. https://doi.org/10.1175/jcli-d-15-0594.1

Wu CH, Hsu HH, Chou MD (2014) Effect of the Arakan Mountains in the northwestern Indochina Peninsula on the late May Asian monsoon transition. J Geophys Res-Atmos 119:10769–10779. https://doi.org/10.1002/2014jd022024

Wu GX, Duan AM, Liu YM, Mao JY, Ren RC, Bao Q, He B, Liu BQ, Hu WT (2015) Tibetan Plateau climate dynamics: recent research progress and outlook. Natl Sci Rev 2:100–116. https://doi.org/10.1093/nsr/nwu045

Wu C-H, Chou M-D, Fong Y-H (2018a) Impact of the Himalayas on the Meiyu-Baiu migration. Clim Dyn 50:1307–1319. https://doi.org/10.1007/s00382-017-3686-x

Wu C-H, Wang S-YS, Hsu H-H (2018b) Large-scale control of the Arabian Sea monsoon inversion in August. Clim Dyn 51:2581–2592. https://doi.org/10.1007/s00382-017-4029-7

Xiaowei H, Riyu L, Shuanglin L (2017) Amplified summer warming in Europe–West Asia and Northeast Asia after the mid-1990s. Environ Res Lett 12:094007

Yim SY, Wang B, Kwon M (2014) Interdecadal change of the controlling mechanisms for East Asian early summer rainfall variation around the mid-1990s. Clim Dyn 42:1325–1333. https://doi.org/10.1007/s00382-013-1760-6

Yu RC, Zhou TJ (2007) Seasonality and three-dimensional structure of interdecadal change in the East Asian monsoon. J Clim 20:5344–5355. https://doi.org/10.1175/2007jcli1559.1

Zhang Q, Wu GX, Qian YF (2002) The bimodality of the 100 hPa South Asia High and its relationship to the climate anomaly over East Asia in summer. J Meteorol Soc Jpn 80:733–744. https://doi.org/10.2151/jmsj.80.733

Zhang PF, Liu YM, He BA (2016) Impact of East Asian summer monsoon heating on the interannual variation of the South Asian high. J Clim 29:159–173. https://doi.org/10.1175/Jcli-D-15-0118.1

Zhou NF, Yu YQ, Qian YF (2009a) Bimodality of the South Asia High Simulated by coupled models. Adv Atmos Sci 26:1226–1234. https://doi.org/10.1007/s00376-009-7219-3

Zhou TJ, Yu RC, Zhang J, Drange H, Cassou C, Deser C, Hodson DLR, Sanchez-Gomez E, Li J, Keenlyside N, Xin XG, Okumura Y (2009b) Why the western Pacific subtropical high has extended westward since the late 1970s. J Clim 22:2199–2215. https://doi.org/10.1175/2008jcli2527.1